悪性脳腫瘍に対する最新放射線治療とその成績
—放射線治療における外科治療の役割—

宮 武 伸 一

Modern Radiotherapy for Malignant Brain Tumors including the Role of Surgery in Radiotherapy

by

Shin-Ichi Miyatake, M.D., Ph.D.

from

Department of Neurosurgery, Osaka Medical College

BNCT has a unique concept for cell biological targeting. BNCT is a binary approach composed of a boron compound and a neutron beam. If we can accumulate boron compounds selectively to tumor tissue, neutron α reaction will occur only within the tumor cells, which is followed by tumor cell death with minimal hazardous effects for normal tissues. We introduce here the indication, clinical results of BNCT for newly diagnosed GBM and recurrent malignant meningiomas. For deep-seated tumors, instilling air into the tumor cavity is useful to obtain deeper neutron flux penetration. In addition, we also introduce how to treat radiation necrosis in the brain. Surgical removal of the necrotic foci and some medical treatments such as anticoagulants and bevacizumab, anti-VEGF antibody, are useful for this treatment.

(Received June 24, 2010; accepted July 5, 2010)

Key words : bevacizumab, BNCT, glioblastoma, malignant meningioma, radiation necrosis

Jpn J Neurosurg (Tokyo) 19 : 899-906, 2010

はじめに

悪性脳腫瘍，ことに悪性グリオーマは，その浸潤性発育のゆえに手術のみでは根治が不可能に近い腫瘍である．最近，テモゾロミド（TMZ）の出現により，化学療法の役割が再認識されている．多施設間の randomized study でグリオブラストーマ（GBM）の生存期間中央値（MST）が 2.5 カ月延長したこと[17]は確かに大きな進歩であり，TMZ+X 線外照射のいわゆる Stupp レジメンが，現在のところ，GBM に対する世界標準治療となっている．しかしながら，裏を返せば，TMZ の併用でも MST の延長は 2.5 カ月にすぎず，化学療法の限界を示すものともいえる．

一方で，悪性グリオーマの補助治療のうち，最も大きな役割を果たしているのは，放射線治療である．影治ら[6]は，第 24 回日本脳神経外科コングレス総会において，過去の報告を詳細にレビューし，悪性グリオーマの標準的放射線治療として，X 線による 1 日 1 回，1 回線量 2 Gy，総線量 60 Gy の分割照射を，MRI での T2 高信号域を照射野とする局所照射が標準的治療として妥当であることを紹介している．多数例の検討により，この標準的放射線治療による MST が 9〜12 カ月という報告が多い[9][20]．また，この治療による画像上の奏効率は 23% と報告されている[1]．少なくとも，新規治療法はこの標準

大阪医科大学医学部脳神経外科／〒569-8686 高槻市大学町 2-7〔連絡先：宮武伸一〕
Address reprint requests to : Shin-Ichi Miyatake, M.D., Ph.D., Department of Neurosurgery, Osaka Medical College, 2-7 Daigaku-machi, Takatsuki-shi, Osaka 569-8686, Japan

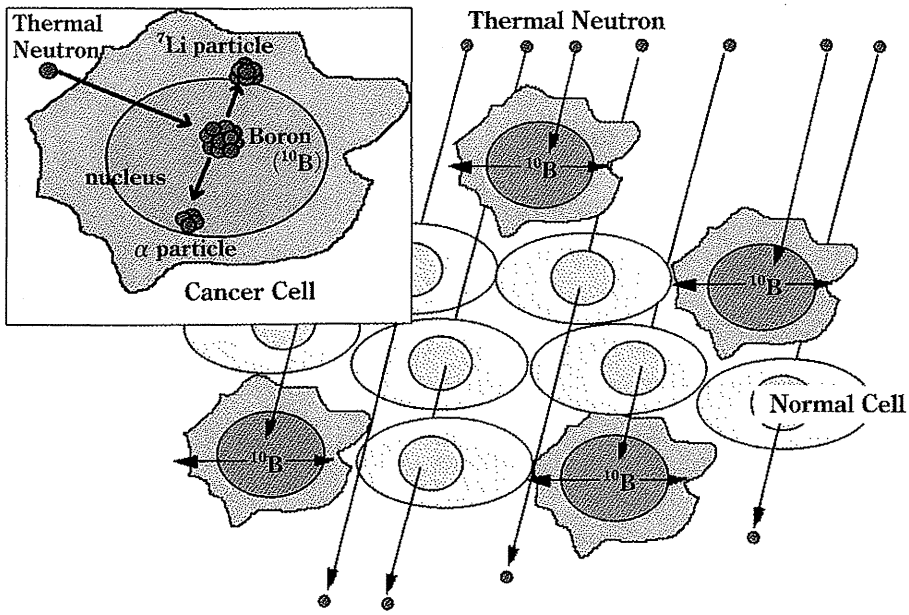

Fig. 1　Principle of BNCT

的治療を上回る成績を残さなければ新しい標準的治療となりえない.

2002年以来, われわれは京都大学原子炉実験所との共同研究を展開し, 85例の悪性脳腫瘍症例に腫瘍選択的粒子線治療であるホウ素中性子捕捉療法（Boron Neutron Capture Therapy：BNCT）を実施してきた. ようやくTMZ導入前の新規診断GBMでの生存解析が可能となり, いまだpreliminaryではあるが, その治療成績をまとめることができるようになった. 本稿ではBNCTの特徴, 適応, 成績を紹介し, 併せて本治療を前提とした外科治療の役割, ならびに副作用として避けて通ることの難しい放射線壊死に対するわれわれの治療法を紹介する.

ホウ素中性子捕捉療法（Boron Neutron Capture Therapy：BNCT）とは

BNCTは原理上腫瘍に対する細胞選択的照射が可能な唯一の放射線治療法である. ホウ素（^{10}B）化合物を投与し, その後, 熱中性子もしくは熱外中性子を照射する. ホウ素化合物自体には細胞毒性はなく, また中性子の殺細胞効果もごく小さいが, ホウ素同位体^{10}B原子核は中性子を捕獲し, きわめて線エネルギー付与（粒子が1μm運動する間に周囲に付与するエネルギー：keV/μm）の高いヘリウム原子核（α粒子）とリチウム反跳核をそれぞれ, 9μmと4μmいう, 細胞1個に相当する距離に放出し, その細胞を破壊する細胞選択的な粒子線治療ともいえる（**Fig. 1**）[2]. すなわち殺細胞効果はホウ素中性子捕獲反応の生じた細胞に限局され, 近隣の細胞には影響を及ぼさない. そこで, ホウ素化合物を腫瘍に選択的に集積できれば, 腫瘍選択的な細胞破壊が可能となる.

BNCTの概念は古く, 1930年代にすでに提唱されており[19], 1950年代には悪性グリオーマに対して, 実際に治療が施行されたが, その結果は満足すべきものではなかった[3]. その原因は深部への中性子線量の不足, 腫瘍と正常脳間のホウ素化合物の濃度比および腫瘍内の絶対濃度が十分でないことが挙げられる. これらの問題を解決すべく, われわれはいくつかの改良を行っている. 中性子の深部到達性を高めるべく, 熱外中性子の利用を開始した. これにより, 非開頭での照射が可能となった. 次いで, 集積機序の異なる2種類の化合物BSH(borocaptate)とBPA (boronophenylalanine)の併用を行っている. BSHは破綻した血液脳関門より受動的に腫瘍組織に移行し, BPAは亢進した蛋白代謝を利用して能動的に腫瘍組織に蓄積される. また, フッ素ラベルしたBPAをトレーサーとして利用することにより, PETにより腫瘍内および脳内BPA濃度が推測され, 治療の適応決定および照射線量がsimulationできる.

悪性グリオーマに対するBNCTの治療効果

Fig. 2に再発GBM症例のBNCT前後の画像を供覧する. 48時間の経過で造影域の70%が消失している[7]. 経験したすべての症例で画像上の改善効果を認め[11], かつ

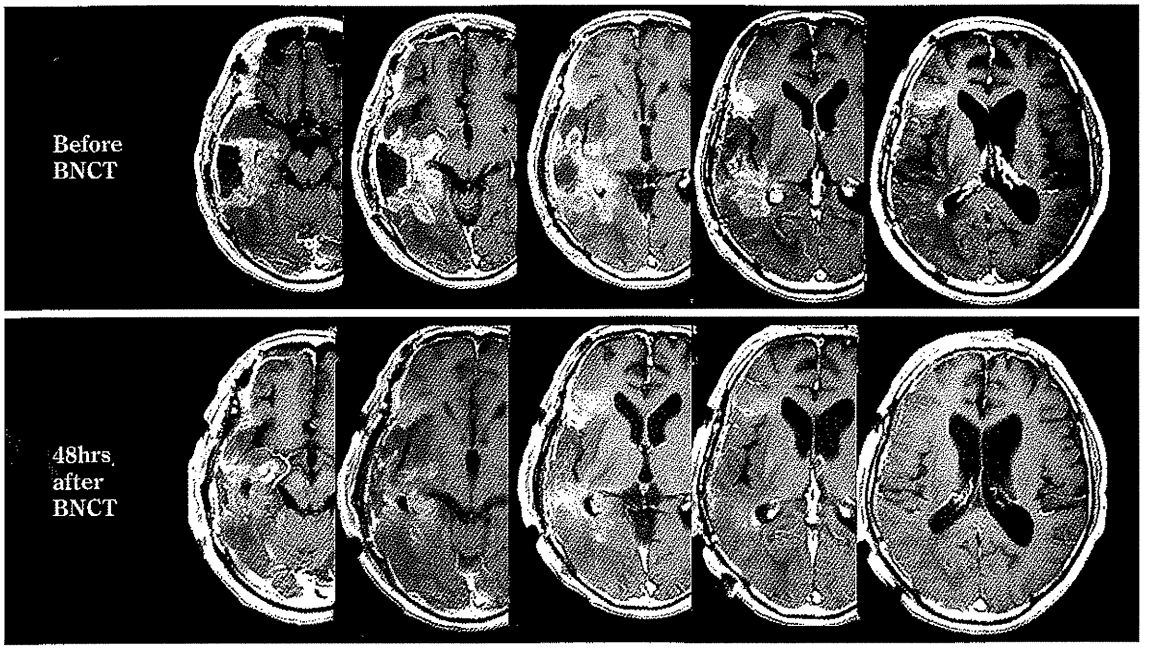

Fig. 2　Early effects of BNCT for recurrent GBM
Seventy % of ehanced mass disappeared in 2 days.

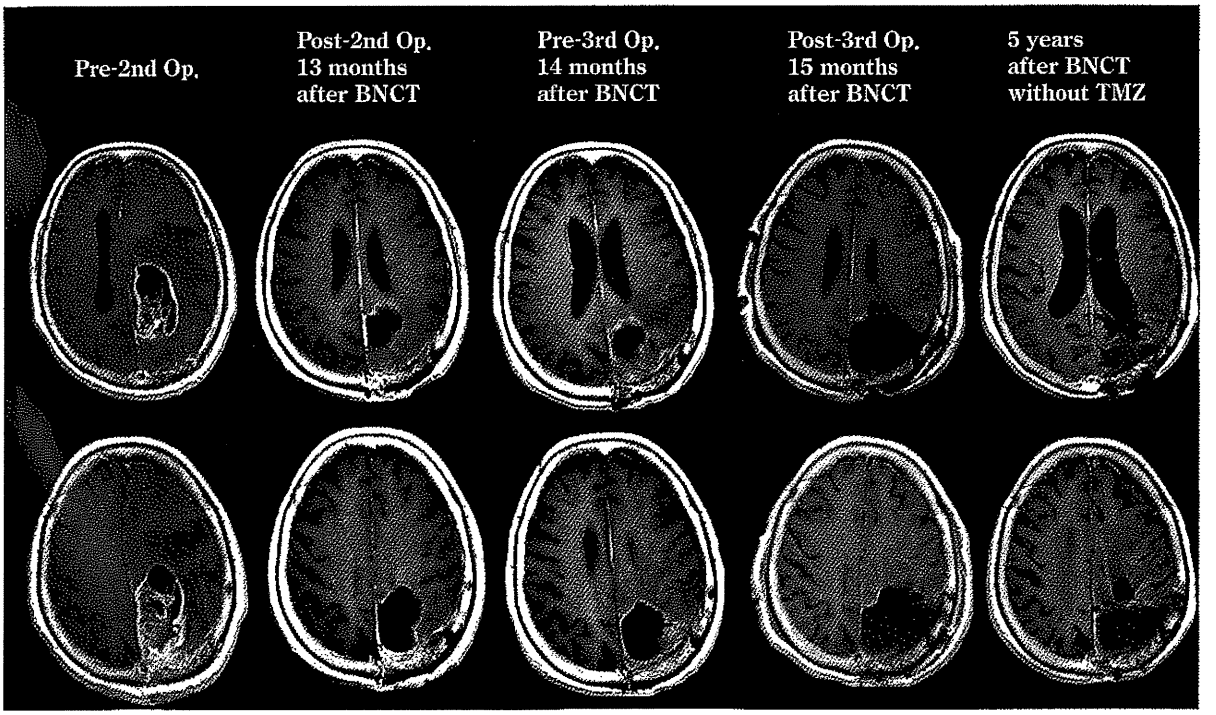

Fig. 3　Periodic change in a newly diagnosed GBM patient after BNCT

多くの症例で BNCT 後に pseudoprogression を経験している[14]．このように，再発例に対しても治療効果を認めたが[7)11)]，前治療として X 線の分割照射が選択されていると，放射線壊死の可能性が高くなり，また，これを避けるため線量不足になる傾向がある．放射線壊死については後述する．

次いで，新規診断 GBM に対する治療効果を紹介する．代表例を **Fig. 3** に供覧する．この症例は左頭頂葉に存在

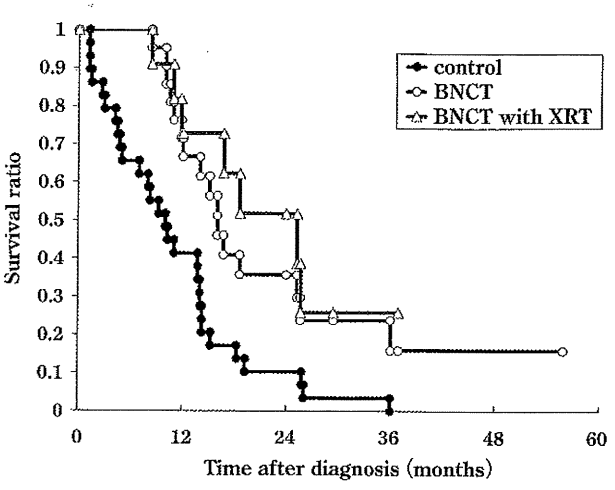

Fig. 4 Survival benefit of newly diagnosed GBM patients treated by BNCT

Closed circle, open circle and open triangle show the overall survaival of historical control, BNCT-treated group and BNCT with XRT-treated groups, respectively.

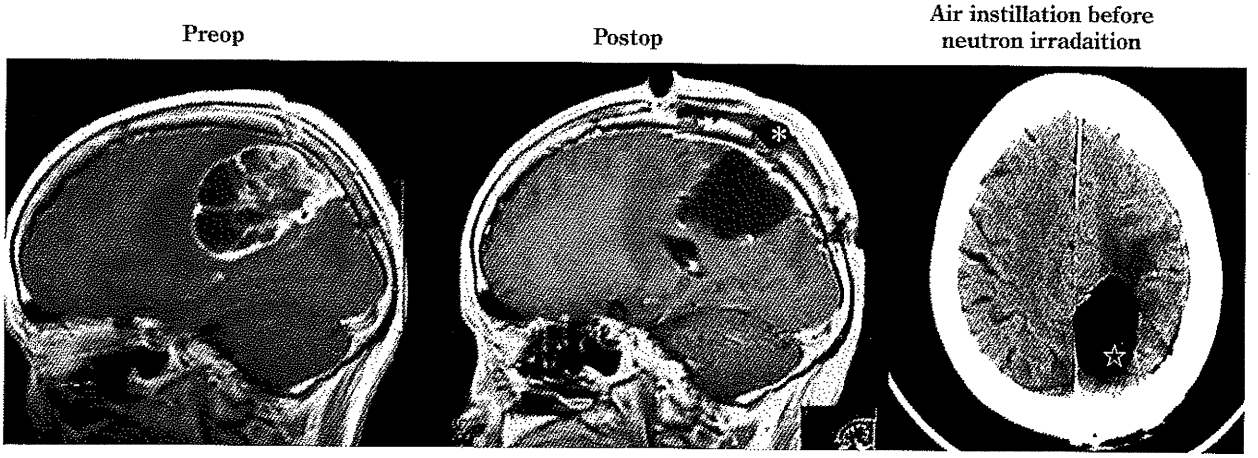

Air instillation	with	without
Minimum tumor dose (Gy-Eq)	26.9	18.9
Maximum brain dose (Gy-Eq)	9.07	12.7

Fig. 5 Effects of air instillation in tumor-removed cavity

＊：Ommaya's reservoir, ☆：air

する最大径 7 cm の GBM であり，近医で生検術のみ行われ，当院に紹介となった．開頭術にて gross total resection を行い，後述の空気置換の後，BNCT を施行．その後，深部線量の不足およびホウ素化合物の不均一分布を補うため 30 Gy の X 線外照射を追加した．

TMZ などの化学療法は追加せず，経過観察を続けていた．BNCT 13 カ月までは何ら症状も画像上増悪もなく経過したが，14 カ月後に造影域の再燃，軽度麻痺の出現を経験し画像上再発の可能性もあり，再開頭により造影域を摘出した．組織は放射線壊死のみであり，腫瘍再発はなく，その後も壊死に対する治療を 2 年続けたのみであり，5 年を経過した現在も再発はない．この症例には再発を疑った段階で 2 回目の BPA-PET を施行し，病変部でのトレーサーの取り込みの低下を確認しており，この症例以降，腫瘍再発と放射線壊死の鑑別に本 PET を活用している[10]．

2007 年までに経験した新規診断 GBM に対する BNCT の治療成績を **Fig. 4** に供覧する．当施設で経験した historical control 27 例，化学療法未施行の BNCT 治療群 21 例，BNCT プラス外照射 11 例の MST はそれぞれ 10.3，15.6，23.5 カ月であり，コントロールと比較して有意な成績を達成することができた[8]．Yamamoto ら[21]もわれわれと同様の治療成績を報告している．TMZ 抜きでは GBM の治療が倫理的に許されない現在，「BNCT+X 線外照射+TMZ」の多施設共同試験を展開中であり，近い将来この成績を公開し，標準治療化の第一歩としたい．

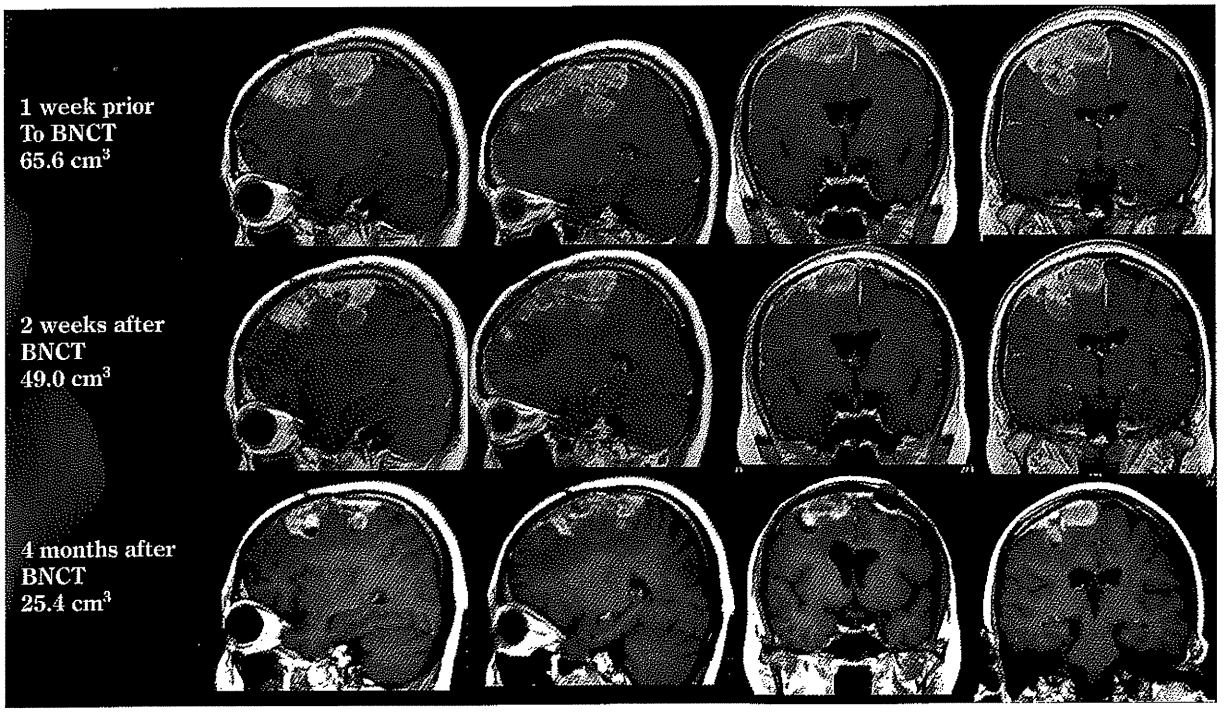

Fig. 6　Concept of BNCT

Effects of BNCT on a recurrent malignant meningioma.
The tumor volume doubled for one month, while waiting for BNCT, which induced hemiparesis. One week after BNCT, she could walk again

また，再発 GBM にも BNCT を積極的に適応し，他の治療では達成できない，再治療後の MST 11 カ月という成績を示している（データ未提示）[15]．再発症例では腫瘍最深部が頭皮より 5 cm 以内であれば，追加切除なしに照射を行っているが，これより深い症例には再摘出のうえ，空気置換を行った後，BNCT を施行している．再発症例ではすでに 60 Gy の X 線外照射が行われており，空気置換により深部腫瘍線量を増加させ，正常脳への吸収線量を減じることがその目的である．しかしながら，BNCT といえど再発例に適応すると，放射線壊死が大きな問題となる．後述のように放射線壊死の治療が奏効すれば再発症例に対する治療成績はさらに伸ばせるものと期待している．

BNCT を前提とした外科治療

残念ながら，GBM では手術による治癒は望めない．また，BNCT にも欠点があり，いかに深部深達性に優れた熱外中性子を使用しても，脳表より 6 cm を超えるような大きな腫瘍に対しては，腫瘍最深部には十分な中性子束の付与は期待しがたい．深部腫瘍に十分な吸収線量を付与しようとすると，正常脳の吸収線量も増加する．そこで Fig. 2 で紹介した患者に用いたわれわれの工夫を紹介する．大型の悪性グリオーマでは腫瘍を可及的に摘出後，腔内に Ommaya's reservoir を設置している（Fig. 5）．中性子照射直前に摘出腔内の髄液を reservoir より排除し，ここを空気で置換した．この操作により腫瘍最深部には空気置換なしに比較して，1.4 倍の吸収線量の付与が可能となり，良好な治療経過に結びついたものと推論している[16]．この症例以降，大型の腫瘍にはこの空気置換を行っている．

悪性髄膜腫に対する BNCT

全髄膜腫のうち数％を占める悪性髄膜腫（WHO grade 3）は GBM 同様きわめて予後不良である．われわれは 15 例の難治性悪性髄膜腫に BNCT を適応し，全例に画像上の改善を認めている[12]．代表例を Fig. 6 に供覧する．5 度の手術，5 回の SRS で制御できなかった悪性髄膜腫であるが，BNCT 直後から歩行障害の改善を認め，腫瘍体積の著減を経験した[18]．ただしこの症例は 2 年後に対側への伸展および全身への転移で亡くなっている．亡くなった症例の多くが全身転移および脳脊髄腔内の播種であり，悪性神経膠腫での播種と同様，解決できていない

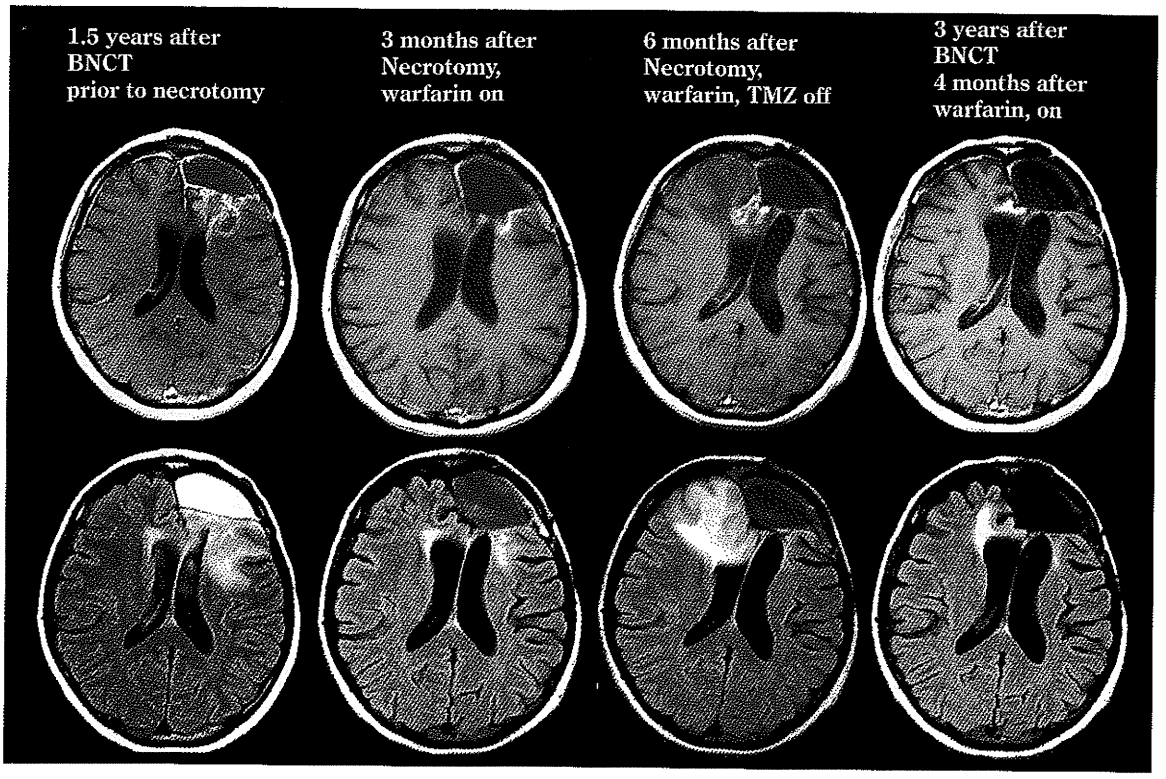

Fig. 7 Effects of surgical removal and anticoagulant therapy on radiation necrosis in the brain

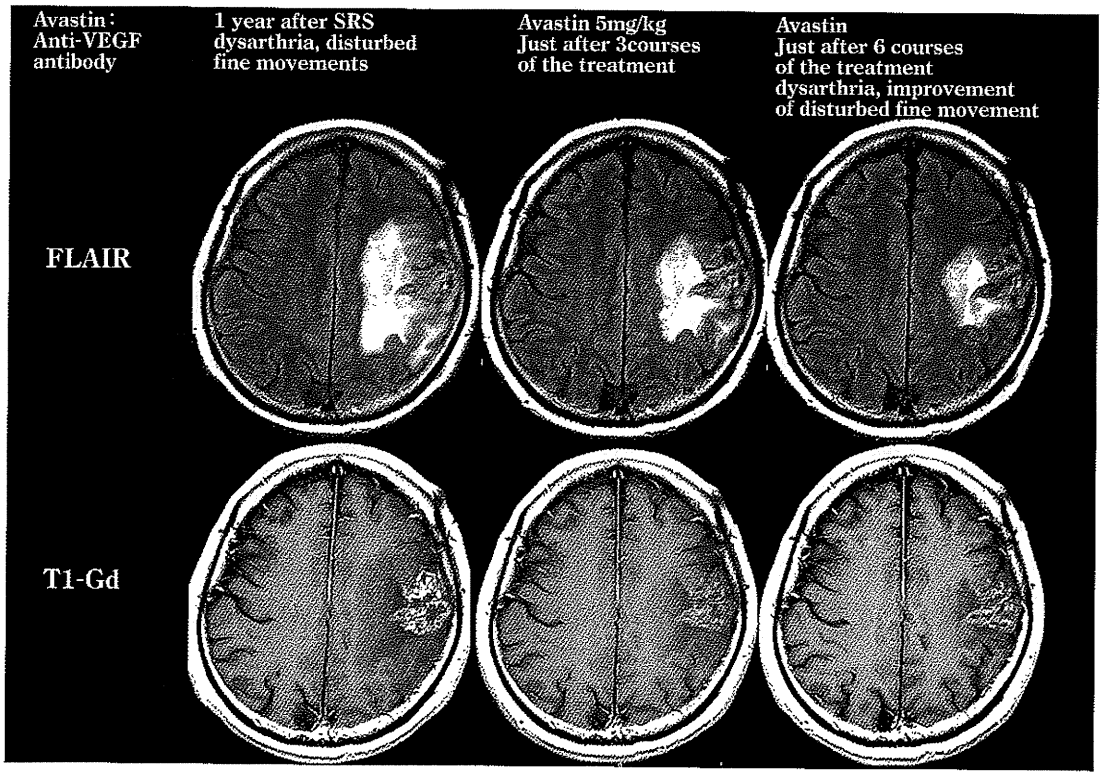

Fig. 8 Effects of bevacizumab on radiation necrosis

大きな問題である[12].

脳放射線壊死に対する外科治療も含めた積極的な治療

BNCT，粒子線治療，強度変調放射線治療，定位放射線治療（SRS）などの高線量放射線治療は，確実に悪性脳腫瘍の生命予後を改善しているが，高線量放射線治療の宿命として脳放射線壊死は避けて通れない大きな問題である．細胞選択的粒子線治療であるBNCTといえども，先行するX線照射歴のある再発症例ではほぼ不可避である．また，造影MRIなどの通常の画像診断では腫瘍進展と放射線壊死との鑑別も困難であり，われわれはBNCTに用いているBPA-PETを両者の鑑別に使用している[10]．この検査により放射線壊死が疑われれば，まず，抗凝固療法等内科的治療を考慮する[4]．この治療に反応せず，症候性となった場合は積極的な壊死巣除去を行っている．また，この壊死巣除去の手術に際して摘出範囲の決定には5-ALAによる蛍光ガイドが有用である[13]．壊死巣除去および抗凝固療法の有効例を供覧する（**Fig. 7**）．この症例では壊死巣除去後も抗凝固療法を続けていたが，妊娠を希望されたため，催奇形性のあるワーファリンおよびTMZを中断しところ，壊死巣の再燃を認め，再度ワーファリンのみ再開し，画像，症状とも落ち着いている．

ただ，症候性放射線壊死に対しても手術による壊死巣摘出が症状の増悪をきたす恐れがある場合や，抗凝固療法が奏効しない症例も多い．最近抗VEGF抗体であるベバシズマブ（商品名アバスチン）が放射線壊死に有効であるとの報告が発表され[5]，われわれも手術不能例には適応している．代表例を**Fig. 8**に供覧する．左運動野に存在する転移性脳腫瘍に対してSRSによる放射線治療後に発症した症候性放射線壊死に対して，5 mg/kgのベバシズマブを2週ごと6回投与した症例の経過である．放射線壊死であるという診断さえ正しければ本治療により，全例改善している．なぜ，壊死巣除去やベバシズマブが浮腫の軽減に有効であるかは現在投稿中であり，別稿で明らかにしたい．また放射線壊死に対するベバシズマブの投与は適応外使用にあたり，現在高度医療として厚生労働省に申請中であることを付記しておく．

おわりに

腫瘍選択的粒子線治療であるBNCTの原理，適応，膠芽腫，悪性髄膜腫に対する治療成績，さらには放射線壊死に対する治療戦略を紹介した．TMZを併用した，新規診断GBMに対する多施設共同研究を展開中であり，より客観的な成績評価が可能となるものと期待する．また，サイクロトロン型小型加速器はすでに完成しており，まもなくこれによる治験を開始する予定である．これが予定どおり稼働すれば，原子炉を必要としない院内BNCTが可能となるものと期待される．

謝　辞

BNCTは脳神経外科医のみで行えるものではない．黒岩敏彦教授以下大阪医科大学脳神経外科のチームの成績であると同時に，終始ご指導をいただいた京都大学原子炉実験所附属粒子線腫瘍学研究センターの小野公二教授のチーム，化合物の開発，供与には大阪府立大学農学部の切畑光統教授のチームに多大なご尽力をいただき，BPA-PETに関しては今堀良夫先生（原籍株式会社CICS）他，西陣病院放射線科のチームにも深謝する．また症例の一部は日本原子力機構研究4号炉で照射を行った．

文　献

1) Barker FG 2nd, Chang SM, Larson DA, Sneed PK, Wara WM, Wilson CB, Prados MD：Age and radiation response in glioblastoma multiforme. *Neurosurgery* **49**：1288-1298, 2001.
2) Coderre JA, Morris GM：Review：The radiation biology of boron neutron capture therapy. *Radiat Res* **151**：1-18, 1999.
3) Farr LE, Sweet WH, Robertson JS, Foster CG, Locksley HB, Sutherland DL, Mendelsohn ML, Stickley EE：Neutron capture therapy with boron in the treatment of glioblastoma multiforme. *Am J Roentgenol Radium Ther Nucl Med* **71**：279-293, 1954.
4) Glantz MJ, Burger PC, Friedman AH, Radtke RA, Massey EW, Schold SC Jr：Treatment of radiation-induced nervous system injury with heparin and warfarin. *Neurology* **44**：2020-2027, 1994.
5) Gonzalez J, Kumar AJ, Conrad CA, Levin VA：Effect of bevacizumab on radiation necrosis of the brain. *Int J Radiat Oncol Biol Phys* **67**：323-326, 2007.
6) 影治照喜，永廣信治：悪性グリオーマに対する放射線治療—治療最前線—．脳外誌 **14**：121-131，2005.
7) Kawabata S, Miyatake S, Kajimoto Y, Kuroda Y, Kuroiwa T, Imahori Y, Kirihata M, Sakurai Y, Kobayashi T, Ono K：The early successful treatment of glioblastoma patients with modified boron neutron capture therapy. Report of two cases. *J Neurooncol* **65**：159-165, 2003.
8) Kawabata S, Miyatake S, Kuroiwa T, Yokoyama K, Doi A, Iida K, Miyata S, Nonoguchi N, Michiue H, Takahashi M, Inomata T, Imahoti Y, Kirihata M, Sakurai Y, Maruhashi A, Kumada H, Ono K：Boron neutron capture therapy for newly diagnosed glioblastoma. *J Radiat Res* (*Tokyo*) **50**：51-60, 2009.
9) Kristiansen K, Hagen S, Kollevold T, Torvic A, Holme I, Nesbakken R, Halltevoll R, Lindgren M, Brun A, Lindgre S, Notter G, Andersen AP, Elgen K：Combined modality therapy of operated astrocytoma gradeIII and IV：Confirmation of the value of postoperative irradiatin and lack of potentiation of bleomycin on survival time：A prospective multicenter trial of the Scandinavian Glioblatoma Study

Group. *Cancer* **47**: 649-652, 1981.
10) Miyashita M, Miyatake S, Imahori Y, Yokoyama, K Kawabata S, Kajimoto Y, Shibata M, Otsuki Y, Kirihata M, Ono K, Kuroiwa T: Evaluation of fluoride-labeled boronophenylalanine-PET imaging for the study of radiation effects in patients with malignant glioblastomas. *J Neurooncol* **89**: 239-246, 2008.
11) Miyatake S, Kawabata S, Kajimoto Y, Aoki A, Yokoyama K, Yamada M, Kuroiwa T, Tsuji M, Imahori Y, Kirihata M, Sakurai Y, Masunaga S, Nagata K, Maruhashi A, Ono K: Modified boron neutron capture therapy (BNCT) for malignant gliomas using epithermal neutron and two boron compounds with different accumulation mechanisms: An efficacy study based on finding on neuroimages. *J Neurosurg* **103**: 1000-1009, 2005.
12) Miyatake S, Tamura Y, Kawabata S, Iida K, Kuroiwa T, Ono K: Boron neutron capture therapy for malignant tumors related to meninigiomas. *Neurosurgery* **61**: 82-91, 2007.
13) Miyatake S, Kuroiwa T, Kajimoto Y, Miyashita M, Tanaka H, Tsuji M: Fluorescence of non-neoplastic, MRI-enhancing tissue by 5-aminolevulenic acid: Report of 3 cases. *Neurosurgery* **61**: E1101-1104, 2007.
14) Miyatake S, Kawabata S, Nonoguchi N, Yokoyama K, Kuroiwa T, Ono K: Pseudoprogression in boron neutron capture therapy for malignant gliomas and meningiomas. *Neuro Onocol* **11**: 430-436, 2009.
15) Miyatake S, Kawabata S, Yokoyama K, Kuroiwa T, Michiue H, Sakurai Y, Kumada H, Suzuki M, Maruhashi A, Kirihata M, Ono K: Survival benefit of boron neutron capture therapy for recurrent malignant gliomas. *J Neurooncol* **91**: 199-206, 2009.
16) Sakurai Y, Ono K, Miyatake S, Maruhashi A: Improvement effect on the depth-dose distribution by CSF drainage and air infusion of a tumour-removed cavity in boron neutron capture therapy for malignant brain tumours. *Phys Med Biol* **51**: 1173-1183, 2006.
17) Stupp R, Mason WP, van den Bent MJ, Weller M, Fisher B, Taphoorn MJB, Belanger K, Brandes AA, Marosi C, Bogdahn U, Curschmann J, Janzer RC, Ludwin SK, Gorlia T, Allgeier A, Lacombe D, Cairncross G, Eisenhauer E, Mirimanoff RO, for the European Organisation for Research and Treatment of Cancer Brain Tumor and Radiotherapy Groups and the National Cancer Institute of Canada Clinical Trials Group: Radiotherapy plus concomitant and adjuvant temozolomide for glioblastoma. *N Engl J Med* **352**: 987-996, 2005.
18) Tamura Y, Miyatake S, Nonoguchi N, Miyata S, Yokoyama K, Doi A, Kuroiwa T, Asada M, Tanabe H, Ono K: Boron neutron capture therapy for recurrent malignant meningioma. Report of first trial. *J Neurosurg* **105**: 898-903, 2006.
19) Tayler HJ, Goldhaber M: Detection of nuclear disintegration in a photographic emulsion. *Nature* **135**: 341, 1935.
20) Walker MD, Green SB, Byar DP, Alexader E Jr, Batzdorf U, Brooks WH, Hunt WE, MacCarty CS, Mahaley MS Jr, Mealey J Jr, Owens G, Ranohoff J 2nd, Robertson JT, Shapiro WR, Smith KR Jr, Wilson CB, Strike TA: Randmized comparison of rdiotherapy and nitrosoureas for the treatment of malignant glioma after surgery. *N Engl J Med* **303**: 1323-1329, 1980.
21) Yamamoto T, Nakai K, Kageji T, Kumada H, Endo K, Matsuda M, Shibata Y, Matsumura A: Boron neutron capture therapy for newly diagnosed glioblastoma. *Radiother Oncol* **91**: 80-84, 2009.

要　旨

悪性脳腫瘍に対する最新放射線治療とその成績
—放射線治療における外科治療の役割—

宮武　伸一

悪性脳腫瘍，ことにグリオーマに対する放射線治療は標準的治療として，1日1回2Gy，総線量60GyのX線分割照射が確立されている．しかしながら，グリオブラストーマに話を限ると，術後この標準的放射線治療を行っても，生存期間中央値（MST）は12カ月であり，夢の新薬といわれたテモゾロミドを併用してもMSTを2.5カ月延長するにすぎず，満足すべき状況とはいえないのが現状である．

第30回日本脳神経外科コングレス総会PS1-1「悪性グリオーマ治療の進歩」では，最新の放射線治療として，陽子線，炭素線などの粒子線治療の特徴と適応ならびに腫瘍選択的粒子線治療であるホウ素中性子捕捉療法（BNCT）の特徴と治療成績，ならびに放射線壊死の治療について紹介を行った．またコングレス総会では「放射線治療における外科治療の役割」という副題をいただいたので，BNCTを前提とした手術の工夫および放射線壊死に対する外科治療を紹介した．本稿では，限られた誌面の都合もあり，BNCTをmainに紹介し，放射線治療における外科治療の役割を述べる．

脳外誌　19：899-906，2010

Gastric Cancer (2010) 13: 264–266
DOI 10.1007/s10120-010-0562-3

Short communication

A case of small undifferentiated intramucosal gastric cancer with lymph node metastasis

Junichirou Nasu[1], Shinichiro Hori[1], Akinori Asagi[1], Tomohiro Nishina[1], Yoshio Ikeda[1], Masahito Tanimizu[1], Haruo Iguchi[1], Kenjiro Aogi[1], Akira Kurita[2], and Rieko Nishimura[3]

[1]Department of Internal Medicine, National Hospital Organization Shikoku Cancer Center, 160 Minamiumemotomachi-Kou, Matsuyama 791-0280, Japan
[2]Department of Surgery, National Hospital Organization Shikoku Cancer Center, Matsuyama, Japan
[3]Department of Clinical Laboratory, National Hospital Organization Shikoku Cancer Center, Matsuyama, Japan

Abstract
Early gastric cancer (EGC) has a favorable prognosis after surgical gastrectomy. For intramucosal EGC with little risk of lymph node metastasis, endoscopic mucosal resection (EMR) is an accepted treatment method. Herein we document a noteworthy case of small undifferentiated gastric cancer with nodal metastasis. A 60-year-old Japanese woman underwent gastrectomy with D2 lymph node dissection for the treatment of EGC in the lower gastric body. Histological examination revealed that signet-ring cell carcinoma was located in approximately one-third of the superficial portion of the mucosal layer, with a tumor size of 13 mm. No lymphatic invasion, venous invasion, or fibrosis was observed in the submucosal layer. This case had nodal metastasis and was finally diagnosed as stage IB (T1N1M0) according to the Japanese Classification of Gastric Carcinoma (JCGC). The patient is alive without recurrence 6 years after treatment.

Key words Early gastric cancer · Lymph node metastasis · Undifferentiated carcinoma

Introduction

Early gastric cancer (EGC) is defined as a gastric cancer localized to the mucosa or submucosa regardless of lymph node metastasis. Radical gastrectomy with regional lymphadenectomy is the gold-standard treatment for patients with EGC [1]. For intramucosal EGC with little risk of lymph node metastasis, endoscopic mucosal resection (EMR) has been accepted as a minimally invasive treatment modality. EMR is generally indicated for intramucosal differentiated adenocarcinoma less than 20 mm in diameter and without ulceration [2, 3]. Recently, several institutions have suggested that the indications for EMR should be expanded to include larger, differentiated intramucosal adenocarcinoma and undifferentiated adenocarcinoma less than 20 mm in diameter and without ulceration.

Offprint requests to: J. Nasu
Received: October 20, 2009 / Accepted: May 19, 2010

Case report

A 60-year-old Japanese woman visited a local hospital because of anorexia and body weight loss, and gastroscopy revealed gastric cancer. She was admitted to our hospital for the treatment of gastric cancer in October 2001. She had no history of malignant disease and no family history of cancer. Upper gastrointestinal endoscopy revealed irregular, depressed mucosa, type 0 IIc in accordance with the *Japanese classification of gastric carcinoma* (JCGC) [4] in the large curvature of the lower gastric body (Fig. 1). The diameter was approximately 1 cm, and there were no ulcer findings. Endoscopic ultrasonography revealed this to be an intramucosal cancer, and computed tomography examination showed no distinct lymph node metastasis. Pathologically, signet-ring cell carcinoma was detected in the biopsy specimen. Laboratory results were within normal limits, and serum carcinoembryonic antigen (CEA) levels were normal. Wedge resection of the stomach with resection of a single lymph node (#4d) was performed in November 2001 (Fig. 2). Histological examination revealed that signet-ring cell carcinoma was located in approximately one-third of the superficial portion of the mucosal layer and that carcinoma cells had not invaded into the muscularis mucosa (Fig. 3A, B). The tumor was 13 mm in size. No lymphatic invasion, venous invasion (immunohistochemical staining with CD34 and D2–40), or ulcer scar was observed in the submucosal layer. Histologically, there was no fibrosis in the submucosal layer and no breakdown of the muscularis mucosa. The resection margin was clear of tumor cells. The single resected lymph node had metastatic cancer cells; these were also signet-ring cell car-

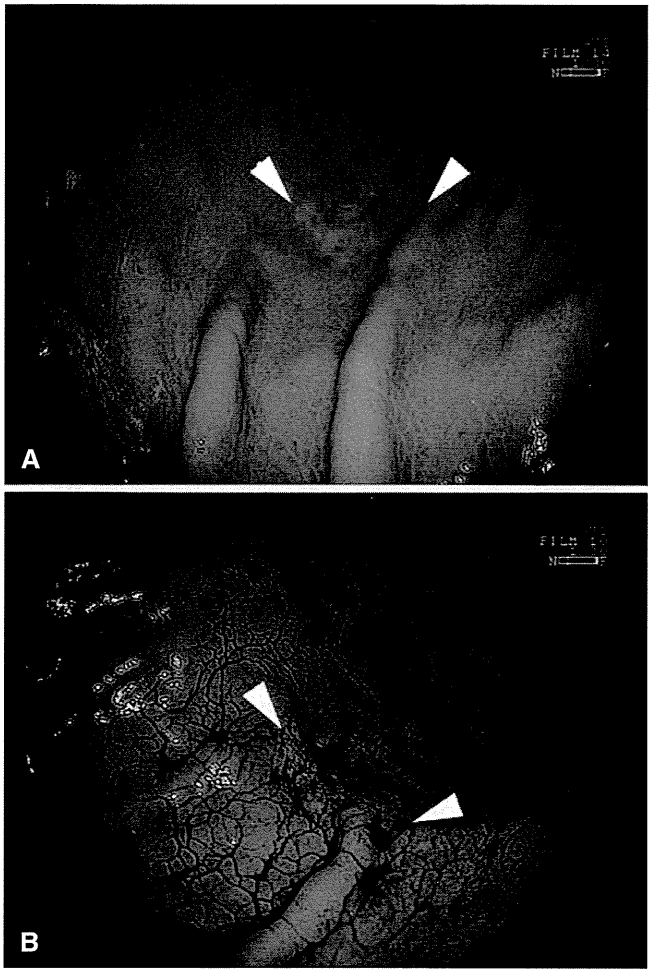

Fig. 1A, B. Gastroscopy revealed a depressed lesion in the large curvature of the lower gastric body (*arrowheads*). There were no ulcer findings, and endoscopic ultrasonography showed that this was an intramucosal cancer. **A** Without dye; **B** dyeing with indigo carmine

cinoma. Immediately, additional distal gastrectomy with D2 lymph node dissection (regional lymph node dissection of all group 1 and group 2 nodes) was performed, with a Billroth-I reconstruction. The gastric body with the first resection scar was histologically examined and there was no cancer lesion. Cancer cell metastasis was detected in nodes #4sb, #4d, and #6 (5/65), and this case was finally diagnosed as stage IB (T1N1M0) according to the JCGC. This patient is alive without recurrence 6 years after treatment.

Discussion

For intramucosal EGC with little risk of lymph node metastasis, EMR is accepted as a minimally invasive treatment modality. Undifferentiated intramucosal EGC is known to be more commonly associated with

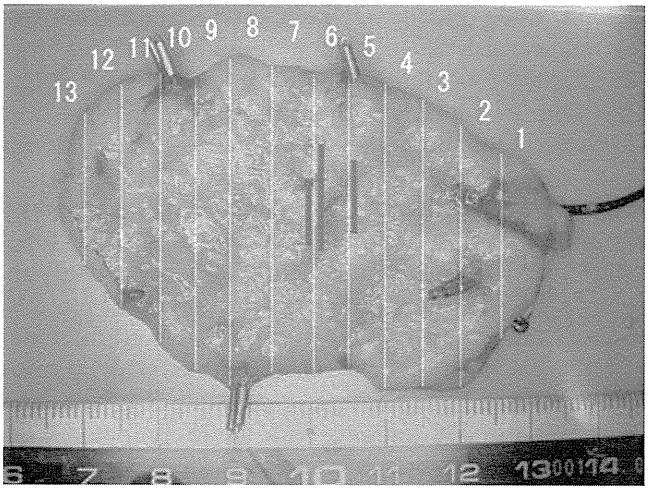

Fig. 2. Surgical specimen from partial gastrectomy. The locations of tumor cells are shown as *bold lines*. The tumor was 13 mm in diameter

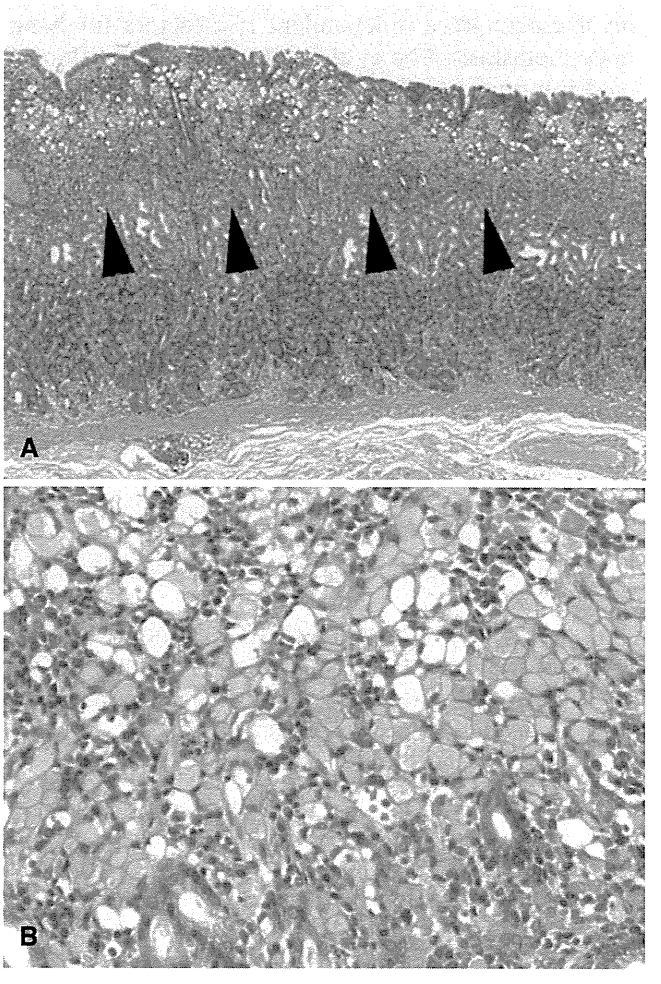

Fig. 3A, B. Histological examination. **A** Signet-ring cell carcinoma was located in approximately one-third of the superficial portion of the mucosal layer, and carcinoma cells had not invaded into the muscularis mucosa. **B** Higher magnification microscopic findings.

lymph node metastasis compared to differentiated intramucosal EGC [5, 6], and the indications for EMR are limited to differentiated intramucosal EGC that is less than 20 mm and without ulceration. Gotoda et al. [3] reported that none of 141 patients with undifferentiated intramucosal EGC less than 20 mm in size without ulceration had lymph node metastasis. The upper limit of the 95% confidence interval was 2.6%, which was considered to be sufficiently large to exclude the possibility of lymph node metastasis. Some predictive factors for lymph node metastasis in undifferentiated EGC have been reported [7–11]. Previously, we retrospectively examined factors predictive of lymph node metastasis in 332 patients with undifferentiated EGC who underwent gastrectomy, including the present patient. Multivariate analysis showed that the presence of lymphatic-vascular involvement was significantly correlated with the incidence of lymph node metastasis [8]. Abe et al. [7] reported that multivariate logistic regression analysis indicated that tumor size and lymphatic involvement were independent risk factors for lymph node metastasis. Abe et al. reported small undifferentiated intramucosal EGC cases with tumors 10, 12, and 20 mm in diameter without ulceration that had lymph node metastasis. These investigators concluded that EMR should not be indicated for undifferentiated EGC more than 10 mm in diameter.

Fewer lymphatic-vascular vessels are present in the mucosal layer than in the submucosal layer. D2-40 immunohistochemical staining has revealed that lymphatic vessels are most densely distributed in the muscularis mucosa layer of the gastric wall [12]. The cancer cells in the patient reported here were located in one-third of the mucosal layer and did not contact the muscularis mucosa. The process of cancer metastasis in this patient is difficult to conjecture. Circulating cancer cells may have played a role, as cancer cells have been identified at the DNA level in the peripheral blood of patients with EGC [13].

The expanded criteria of EMR for undifferentiated EGC are controversial. For further clarification of this issue, prognostic data for patients with undifferentiated EGC treated by EMR are required.

Acknowledgments This study was supported in part by a Grant-in-Aid for Cancer Research (21–2) from the Japanese Ministry of Health, Labour and Welfare.

References

1. Okamura T, Tsujitani S, Korenaga D, Haraguchi M, Baba H, Hiramoto Y, et al. Lymphadenectomy for cure in patients with early gastric cancer and lymph node metastasis. Am J Surg 1988;155: 476–80.
2. Yamao T, Shirao K, Ono H, Kondo H, Saito D, Yamaguchi H, et al. Risk factors for lymph node metastasis from intramucosal gastric carcinoma. Cancer 1996;77:602–6.
3. Gotoda T, Yanagisawa A, Sasako M, Ono H, Nakanishi Y, Shimoda T, et al. Incidence of lymph node metastasis from early gastric cancer: estimation with a large number of cases at two large centers. Gastric Cancer 2000;3:2 19–25.
4. Japanese Gastric Cancer Association. Japanese classification of gastric carcinoma — 2nd English edition —. Gastric Cancer 1998;1:10–24.
5. Wu CY, Chen JT, Chen GH, Yeh HZ. Lymph node metastasis in early gastric cancer: a clinicopathological analysis. Hepatogastroenterology 2002;49:1465–8.
6. Hyung WJ, Cheong JH, Kim J, Chen J, Choi SH, Noh SH. Application of minimally invasive treatment for early gastric cancer. J Surg Oncol 2004;85:181–5; discussion 6.
7. Abe N, Watanabe T, Sugiyama M, Yanagida O, Masaki T, Mori T, et al. Endoscopic treatment or surgery for undifferentiated early gastric cancer? Am J Surg 2004;188:181–4.
8. Nasu J, Nishina T, Hirasaki S, Moriwaki T, Hyodo I, Kurita A, et al. Predictive factors of lymph node metastasis in patients with undifferentiated early gastric cancers. J Clin Gastroenterol 2006; 40:412–5.
9. Li C, Kim S, Lai JF, Oh SJ, Hyung WJ, Choi WH, et al. Risk factors for lymph node metastasis in undifferentiated early gastric cancer. Ann Surg Oncol 2008;15:764–9.
10. Ye BD, Kim SG, Lee JY, Kim JS, Yang HK, Kim WH, et al. Predictive factors for lymph node metastasis and endoscopic treatment strategies for undifferentiated early gastric cancer. J Gastroenterol Hepatol 2008;23:46–50.
11. Park YD, Chung YJ, Chung HY, Yu W, Bae HI, Jeon SW, et al. Factors related to lymph node metastasis and the feasibility of endoscopic mucosal resection for treating poorly differentiated adenocarcinoma of the stomach. Endoscopy 2008;40:7–10.
12. Sako A, Kitayama J, Ishikawa M, Yamashita H, Nagawa H. Impact of immunohistochemically identified lymphatic invasion on nodal metastasis in early gastric cancer. Gastric Cancer 2006;9:295–302.
13. Koga T, Tokunaga E, Sumiyoshi Y, Oki E, Oda S, Takahashi I, et al. Detection of circulating gastric cancer cells in peripheral blood using real time quantitative RT-PCR. Hepatogastroenterology 2008;55:1131–5.

Full Paper

CONTRAST MEDIA & MOLECULAR IMAGING

Received: 15 February 2009, Revised: 7 December 2009, Accepted: 16 December 2009, Published online in Wiley InterScience: 16 March 2010

(www.interscience.wiley.com) DOI:10.1002/cmmi.367

E-selectin targeting to visualize tumors in vivo

Masahiko Hirai[a,b], Yoshie Hiramatsu[a], Shinki Iwashita[a], Takayuki Otani[a,b], Ling Chen[b], Yue-guang Li[b], Masashi Okada[b], Kazunori Oie[a], Koich Igarashi[a], Hideaki Wakita[c] and Masaharu Seno[b]*

Generally angiogenic factors induce the expression of E-selectin in vascular endothelial cells in the tumors. In this study, we employed an anti-E-selectin monoclonal antibody to target tumors *in vivo* and evaluated an optical imaging reagent to visualize tumor regions. The anti-E-selectin antibody was conjugated on the surface of liposomes, which encapsulated the near-infrared fluorescent substances Cy3 or Cy5.5. The liposomes efficiently recognized human umbilical vein endothelial cells only when E-selectin was induced by angiogenic factors such as TNF-α *in vitro*. Cy5.5 encapsulated into liposomes that were conjugated with an anti-E-selectin antibody successfully visualized Ehrlich ascites tumor cells when transplanted into mice. Thus, E-selectin targeting with liposomes containing a near-infrared fluorescent dye was found effective in visualizing tumors *in vivo*. This strategy should be extremely useful as a method to identify sentinel lymphatic nodes and angiogenic tumors as well as use for drug delivery to tumor cells.

Keywords: Liposome; E-selectin; *in vivo* imaging; drug delivery system

1. INTRODUCTION

The field of non-invasive *in vivo* imaging is rapidly growing with new technologies and techniques. Near-infrared fluorescent substances are being utilized for *in vivo* imaging of small animals because the near-infrared region of the spectrum offers certain advantages for photon penetration and because both organic and inorganic fluorescence contrast agents are now available for chemical conjugation to targeting molecules (1). Liposomes are currently being utilized as carriers for delivering various drugs and substances. For passive delivery both the size and electric charge of the surface of liposomes have to be carefully optimized to deliver agents to the proper targets (2–4). Various molecules such as antibodies, transferrin, folic acid and monosaccharide have been conjugated to the surface of liposomes but few have been successful for targeting tumor cells (4,5). Taking this into consideration, we reasoned that the E-selectin ligand might confer potential tumor targeting to liposomes (6,7). E-selectin is expressed on tumor vascular endothelial cells that have been stimulated by cytokines such as TNF-α, IL1-β and VEGF (8–13). While there are 14 lectin categories, which are classified by their primary structure, including C-type lectin, galectin, I-type lectin, P-type lectin and pentraxin (14–16), E-selectin belongs to the C-type lectin family and is well characterized in inflammation and in tumors. Liposomes that have been conjugated with an anti-E-selectin antibody can successfully target cells that are expressing E-selectin *in vitro* (17–20). However, *in vivo* targeting with liposomes conjugated with such an antibody has not been successful because liposomes are rapidly depleted *in vivo* after being entrapped by the reticular endothelial system (RES) in the liver and spleen or by binding to opsonin proteins in blood and then phagocytosed by macrophages (4,5,17). More extended retention in the blood vessels appears to be necessary for binding to endothelial cells on which E-selectin is expressed.

In this report, we describe a method for targeting tumor cells *in vivo* for imaging using a near-infrared fluorescent dye which has been encapsulated into liposomes which are conjugated to anti-E-selectin antibody and which have been negatively charged with a hydrophilic substance.

2. RESULTS

2.1. Properties of liposomes

Cy3 or Cy5.5 encapsulated liposomes were conjugated with anti-E-selectin antibody (Fig. 1). The surface of the liposomes was modified to possess a negative charge so that repulsive forces between the liposomes and the wall of blood vessels would reduce non-specific binding of the liposomes *in vivo*. The final concentration of lipid of the liposomes encapsulating Cy5.5 was in the range from 2.5 to 3.0 mg/ml and the concentration of Cy3 was from 2.7 to 3.1 mg/ml. As summarized in Table 1, the mean particle size of the liposome population was approximately 90 nm, which was not affected by either the type of dye that was encapsulated or the quantity of antibody that was conjugated on

* *Correspondence to: M. Seno, Rm361, Bldg ENG-6, Department of Medical and Bioengineering Science, Graduate School of Natural Science and Technology, Okayama University, 3.l.1 Tsushima-naka, Kita-ku, Okayama 700-8530, Japan. E-mail: mseno@cc.okayama-u.ac.jp*

a *M. Hirai, Y. Hiramatsu, S. Iwashita, T. Otani, K. Oie, K. Igarashi*
R&D Division, Katayama Chemical Industries Co. Ltd, Minoh, Osaka 562-0015, Japan

b *M. Hirai, T. Otani, L. Chen, Y.-g. Li, M. Okada, M. Seno*
Laboratory of Nano-Biotechnology, Department of Medical and Bioengineering Science, Graduate School of Natural Science and Technology, Okayama University, 3.1.1 Tsushima-Naka, Kita-ku, Okayama 700-8530, Japan

c *H. Wakita*
Section of Prevention and Therapy, Department of Vascular Dementia Research, National Institute for Longevity Sciences, National Center for Geriatrics and Gerontology, Obu, Aichi 474-8511, Japan

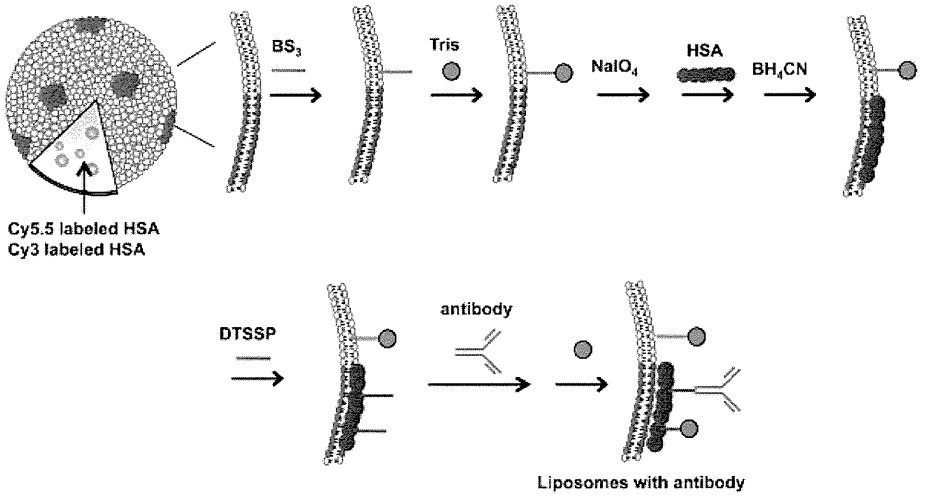

Figure 1. Preparation scheme of liposomes conjugated with antibody. First of all, Cy3 or Cy5.5 conjugated with human serum albumin (HSA) was encapsulated in the hydrophilic anionic liposomes. Then tris(hydroxymethyl)aminomethane (Tris) was crosslinked on the liposomes surface via bis(sulfosuccinimidyl)suberate (BS_3). HSA was bound to the ganglioside component of liposomes. Finally, anti-E-selectin antibody was conjugated to HSA via DTSSP.

the surface. The ζ-potential, which reflects the surface electric charge of the liposome membrane, was approximately −60 mV (Table 1). The size distribution of the liposomes did not show any changes during 6 months of storage at 4°C.

2.2. Concentrations of antibody conjugated to liposomes

Various concentrations of antibody were assessed to optimize the efficiency of conjugation between liposomes and anti-E-selectin antibody (Table 1). The amount of antibody bound to the surface of the liposomes increased depending on the concentration of antibody in the reaction. As described below, the optimal amount of antibody bound to the surface of liposomes was over 3.9 μg/mg lipid for *in vivo* imaging experiments such that the concentration of antibody in the reaction should be approximately 75 μg/mL or more.

2.3. Expression of E-selectin on vascular endothelial cells after treatment with Ehrlich ascites tumor (EAT)-conditioned medium

In vascular endothelial cells, E-selectin is induced by inflammatory cytokines or angiogenic factors such as IL1-β, TNF-α and VEGF where it is not usually expressed (8–13). This induction was confirmed on human umbilical vein endothelial cells (HUVEC) stimulated with TNF-α in serum-free conditions (Fig. 2). Although culture medium containing fetal bovine serum (FBS) did not induce E-selectin expression, the conditioned medium of EAT

Table 1. Physicochemical properties of liposomes conjugated with anti-E-selectin antibody

	Antibody concentration in conjugating reaction (μg/ml)						
	0	25	50	75	100	200	300
Cy5.5 encapsulated liposomes (n = 3)							
Diameter (nm)	82 ± 2	82 ± 4	82 ± 4	91 ± 3	86 ± 4	84 ± 3	86 ± 2
ζ-Potential (mV)	−56 ± 4	−59 ± 4	−58 ± 5	−55 ± 8	−60 ± 8	−49 ± 9	−51 ± 6
Lipid concentration (mg/ml)	2.5 ± 0.2	2.9 ± 0.1	3.0 ± 0.2	2.8 ± 0.1	2.8 ± 0.2	2.7 ± 0.2	2.7 ± 0.2
Absorbance at 680 nm	2.0	1.9	2.2	1.8	1.7	1.6	1.8
Antibody bound to liposomes (μg/mg lipid)	0	1.0 ± 0.2	2.7 ± 0.4	3.9 ± 0.7	4.5 ± 0.6	6.2 ± 0.8	7.6 ± 0.5
Cy3 encapsulated liposomes (n = 3)							
Diameter (nm)	87 ± 4	85 ± 4	89 ± 3	82 ± 2	ND[a]	ND	ND
ζ-Potential (mV)	−60 ± 2	−59 ± 4	−63 ± 5	−52 ± 6	ND	ND	ND
Lipid concentration (mg/ml)	2.8 ± 0.3	3.1 ± 0.1	2.7 ± 0.1	2.9 ± 0.4	ND	ND	ND
Absorbance at 580 nm	2.8	2.5	2.6	2.4	ND	ND	ND
Antibody bound to liposomes (μg/mg lipid)	0	1.2 ± 0.3	2.5 ± 0.5	3.9 ± 0.4	ND	ND	ND

[a]Not determined.

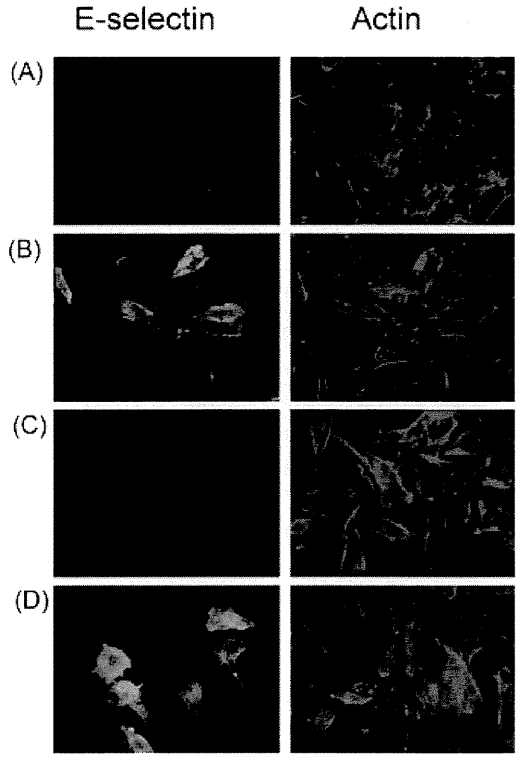

Figure 2. Induction of E-selectin expression in HUVEC. HUVEC were cultured in medium (A), with 10 ng/ml of TNF-α (B), with the fresh medium prepared for EAT cells (C) and with the conditioned medium of EAT cells (D). To detect E-selectin, anti-E-selectin antibody was used followed by FITC labeled anti-mouse IgG antibody. Actin filaments were stained with rhodamine phalloidin. Magnification was × 40.

cells induced the expression of E-selectin in HUVEC, suggesting that EAT cells secretes cytokines or factors stimulating E-selectin expression in HUVEC.

2.4. Visualization of vascular endothelial cells by targeting E-selectin in vitro

Liposomes that had been conjugated to an anti-E-selectin antibody were added to the culture medium of HUVEC that was expressing E-selectin. Since fluoresce of Cy3 is stronger than that of Cy5.5 *in vitro*, liposomes encapsulating Cy3 were used in this experiment. As shown in Fig. 3, HUVEC were visualized by the fluorescent signal of Cy3 only when the liposomes were conjugated with antibody against E-selectin. The specific binding of liposomes to E-selectin was assessed in the presence of an excess amount of free anti-E-selectin antibody. As a result, the fluorescence of liposomes was completely abrogated (Fig. 3C).

2.5. Expression of E-selectin on vascular vessel in EAT

To confirm the expression of E-selectin on vascular vessels in EAT tumor tissues, tumors were excised 10 days after transplantation and tissue sections were prepared, fixed and stained for E-selectin with FITC labeled anti-E-selectin antibody. Additionally, vessels were stained with *Lycopersicon esculentum* (tomato) lectin, which recognizes specifically fucose on the vascular endothelial cells (21). The expression sites of E- selectin staining in the tumor tissue were within the regions of vascular endothelials (Fig. 4). This demonstrates that the expression of E-selectin was induced on blood vessels endothelial cells in EAT tumor tissues. Collectively with the *in vitro* data, these results suggest that EAT cells should secrete cytokines or factors which can induce E-selectin expression in mouse vascular endothelial cells (Fig. 2).

2.6. Visualization of tumors by targeting E-selectin in vivo

To assess if tumor *in vivo* could be visualized, liposomes conjugated with anti-E-selectin antibody in the range from 0 to 7.6 μg antibody/mg lipid of liposome were injected into EAT-bearing mice via the tail vein. Liposomes encapsulating Cy5.5, which has an emission wavelength at 650 nm, which is superior in photon penetration to that of Cy3, were used to monitor the delivery from outside of the body. The time course change of fluorescence intensity from the tumor, which was transplanted into the right femoral region, was monitored as photon counts per second up to 96 h (Fig. 5). An increase in photon counts in tumors was observed from 24 to 96 h after injection with liposomes conjugated to the antibody. The tumor-specific accumulation of liposomes was less significant when the conjugated antibody was less than 3.9 μg/mg lipid. At least 3.9 μg/mg lipid of antibody was required to observe antibody-directed tumor-specific accumulation of liposomes. The increased photon counts in the tumor continued up to 96 h after injection but did not correlate with the amounts of antibody in the range between 3.9 and 7.6 μg antibody/mg lipid. Although a simple passive level of accumulation was also detectable when liposomes without anti-E-selectin antibody were injected, *in vivo* imaging of tumors was only successful when the liposomes were conjugated with anti-E-selectin antibody (Fig. 6).

3. DISCUSSION

Vascular endothelial cells in solid EAT should conceivably be stimulated to express E-selectin *in vivo* as well as *in vitro* (Fig. 2 and 4), resulting in the tumor specific accumulation of liposomes with anti-E-selectin antibody. In our previous study, when liposomes were conjugated with sialyl Lewis^X (SLX), the fluorescence in tumors achieved a maximum at 48 h after injection and then gradually decreased by 96 h after injection (22). In contrast, photon counts of fluorescence from Cy5.5-labeled liposomes in the tumors increased during 72 h and were maintained at a high level up to 96 h after injection when the liposomes were conjugated with anti-E-selectin antibody. The high affinity of liposomes to E-selectin might account for the difference in retention time of fluorescence between the SLX and anti-E-selectin antibody. Monovalent SLX to E-selectin is very weak (K_d, mM) relative to the affinity of antibody to E-selectin (K_d, nM), which results in efficient uptake into tumor tissue (23). Thus longer retention times of liposomes in tumors could be expected when liposomes are conjugated to anti-E-selectin antibody. Considering the fact that pin-point active targeting *in vivo* has been extremely difficult so far (4,5,17), the modification of the liposome surface with a negative charge that was used in this study should also be important. We introduced a negative charge on the surface of liposomes since this modification allowed liposomes that had been conjugated

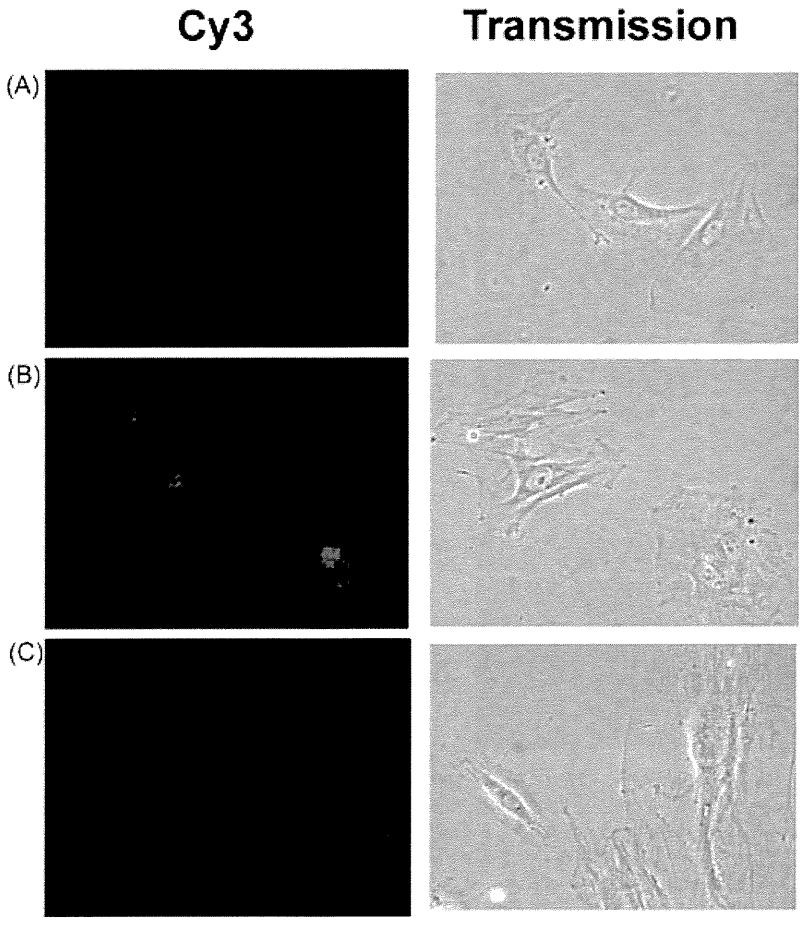

Figure 3. Binding of Cy3-liposomes conjugated with anti-E-selectin antibody to HUVEC. HUVEC was stimulated with TNF-α in advance to express E-selectin. Cy3-liposomes without anti-E-selectin antibody (A) or with anti-E-selectin antibody (3.9 μg/mg lipid) (B) were incubated with HUVEC expressing E-selectin at 37 °C for 30 min, respectively. E-selectin on HUVEC was masked with unlabeled anti-E-selectin antibody by incubation for 30 min prior to the incubation with Cy3-liposomes with anti-E-selectin antibody (3.9 μg/mg lipid) for 30 min (C). Cells were observed under a fluorescence microscope. Magnification was × 40.

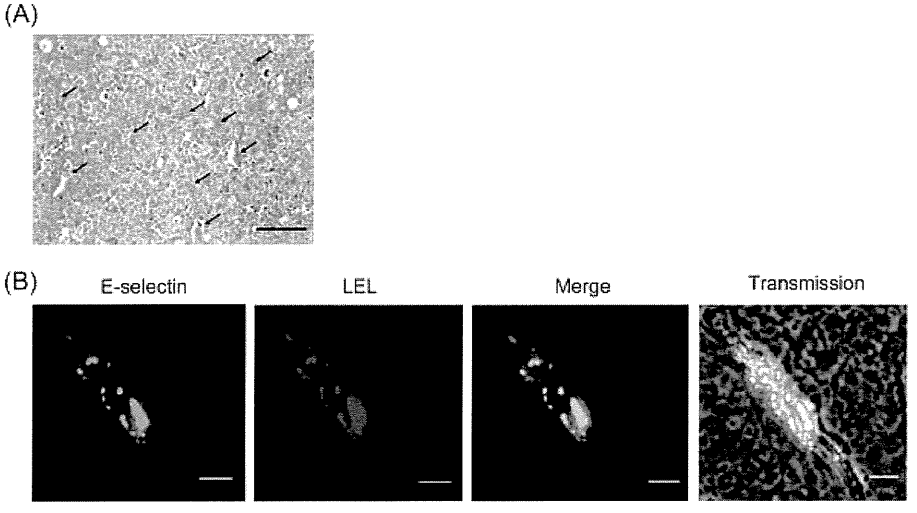

Figure 4. The expression of E-selectin in vascular vessels of solid EAT section. (A) Several vascular vessels (arrows) were observed in HE staining section in one visual field. Scale bar: 100 μm. (B) Double staining of the blood vessel for E-selectin and *Lycopersicon esculentum* lectin (LEL). After deparafinized, the sections were incubated with anti-E-selectin antibody (10 μg/ml) for 1 h at 37 °C, then incubated with goat anti-mouse FITC IgG secondary antibody (green fluoresence) and Texas red conjugated LEL (Red fluoresence) for 1 h at room temperature. Scale bar: 20 μm.

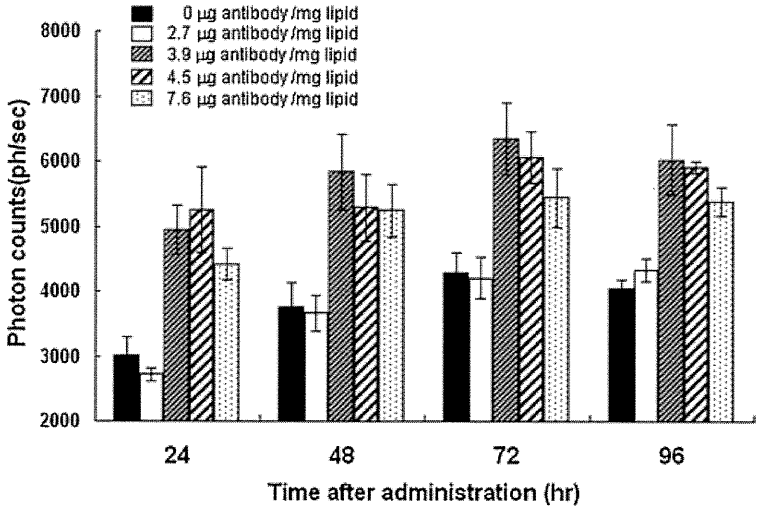

Figure 5. Accumulation of Cy5.5-liposomes conjugated with anti-E-selectin antibody in tumor regions. Cy5.5-liposomes conjugated with anti-E-selectin antibody at 0, 2.7, 3.9, 4.5 and 7.6 μg antibody/mg lipid were injected from the tail veins of EAT tumor-bearing mice. The fluorescence excited at 680 nm was detected as emission spectrum at 700 nm from the tumor region of the same mouse after 24, 48, 72 and 96 h of injection and photons per second were counted. Each vertical bar indicates mean ± SD at $n = 3$.

with antibody to have a long half-life in blood resulting in efficient and active targeting of tumors *in vivo* (24–27). Simultaneously, a hydrophilic surface is established on the liposomes. The repulsive force between the liposomes and the wall of blood vessels should enhance the retention in the vascular system. All of these modifications might assist the liposomes for *in vivo* imaging of tumor by targeting E-selectin and escaping from RES, opsonin proteins in blood plasma and uptake by phagocytotic macrophages. However, *in vivo* imaging from the abdominal side of the animal showed high fluorescence in the liver 72 h after administration (data not shown). As a result, efficient and specific accumulation of liposome-conjugated antibodies could be observed in the final target region with the exception of the liver.

Here we successfully demonstrated visualization of tumors, in which tumor-associated vascular endothelial cells were expressing E-selectin presumably as a consequence of angiogenic factors that were secreted from the tumor, with liposomes conjugated to an anti-E-selectin antibody. Although we did not evaluate an inflammatory model in this report, E-selectin should also be expressed on endothelial cells in inflammatory regions. Recently, nanoparticles conjugated with SLX which were designed for MRI imaging have been reported to image regions of inflammation in the brain for a short time (28). In this context, E-selectin targeting should also be useful for visualization of inflammatory regions *in vivo*. While it is important to distinguish these two different states of tissues, E-selectin targeting should be significantly useful for diagnosis and treatment since inflammation is a well-known risk factor for tumor development and correlates with increased invasiveness and prognosis in a variety of cancers (29). In this report, the maximum accumulation of liposomes conjugated with anti-E-selectin antibody in tumors was achieved 72 h after administration. The accumulation of the liposomes started right after administration and the tumor region could be visualized even 1 h after administration. However, the background was still higher, presumably due to the majority of liposomes circulating in blood vessels.

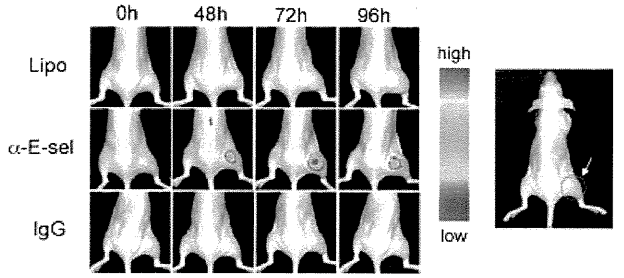

Figure 6. *In vivo* imaging of tumor regions targeting E-selectin. Cy5.5-liposomes without antibody (Lipo), Cy5.5-liposomes conjugated with non-specific porcine antibody at 3.9 μg antibody/mg lipid (IgG) or Cy5.5-liposomes conjugated with anti-E-selectin antibody at 3.9 μg antibody/mg lipid (α-E-sel) were injected into the tail veins of EAT tumor bearing mice. The white arrow indicates tumor region. Images of fluorescence excited at 680 nm were detected as emission spectra at 700 nm in the tumor regions. Each panel was observed at 48, 72 and 96 h after injection.

4. CONCLUSIONS

In this report we have successfully shown that the liposomes conjugated with an anti-E-selectin antibody are available as efficient and specific vectors for imaging *in vivo* targeting to tumor regions. Therefore, the liposomes conjugated with an anti-E-selectin antibody should also be useful as a drug delivery vector of anti-cancer agents. Very recently, lymphatic endothelium has been reported to be sensitive to chemokines for induction of E-selectin *in vitro* (30). The liposomes described in this study might be useful for the identification of sentinel lymphatic nodes. Furthermore, efficient encapsulation of anti-cancer agents into these liposomes should lead to the development of a novel therapeutic technology targeting neovascularization induced by the cytokines secreted from tumors. Since a number of antigens

specific to cancers and other diseases are now being extensively evaluated in various fields, the choice of suitable antibodies specific to these antigens would allow proper delivery of liposomes for therapy. In this context, the present technology should be useful as an active and selective targeting drug delivery system conveying chemical compounds, proteins and nucleic acids, as well as *in vivo* imaging reagents to tumors.

5. EXPERIMENTAL PROCEDURES

5.1. Preparation of anti-E-selectin monoclonal antibody

Female BALB/c mice (6 weeks old) were purchased from Japan SLC. Five hundred micrograms per mouse of pristine (Sigma-Aldrich) was administered twice into the peritoneal cavity of mice with a 5-day interval. At 5 days after the second administration of pristine, 1×10^7 cells of CCL-3 hybridoma (ATCC) producing anti-E-selectin monoclonal antibody were transplanted into the peritoneal cavity. After 20 days, ascites fluid was collected. Ammonium sulfate precipitation was then performed, and the antibody was purified using an affinity purification system (HiTrap Protein G columns, GE Healthcare).

5.2. Preparation of liposomes conjugated with antibody

Preparation of hydrophilic anionic liposomes and encapsulation of Cy3 or Cy5.5 were carried out as described previously (22). The concentration of Cy dye was estimated according to the absorbance at 580 nm for Cy3 and at 680 nm for Cy5.5 measured by Ultrospec 6300 pro (Amersham Biosciences). These liposomes were basically composed of dipalmitoylphosphatidylcholine (DPPC), dipalmitoylphosphatidylethanolamine (DPPE), dicetylphosphate (DCP), cholesterol and ganglioside. DCP was used to confer a negative charge to the liposome surface. Tris(hydroxymethyl)aminomethane (Tris) was crosslinked on the liposome surface via bis(sulfosuccinimidyl)suberate (BS_3; Pierce) to confer hydrophilicity. Using 3,3′-dithiobis(sulfosuccinimidyl)propionate (DTSSP; Pierce), the anti-E-selectin antibody was crosslinked to human serum albumin (HSA; Sigma), which was then coupled in advance to the ganglioside component of liposomes as described previously (22). Anti-E-selectin monoclonal antibody was added to a final concentration of 50, 75, 100, 200 or 300 μg/ml and stirred at 25°C for 2 h. Tris–HCl was then added to reach a final concentration of 132 mg/mL, and stirred overnight at 4°C for hydrophilization of the liposome surface (Fig. 1). As a control, liposomes without antibody and liposomes conjugated with IgG (porcine) were also prepared. IgG was added to a final concentration of 75 μg/ml. The preparation of liposome without antibody was the same as in the case of antibody-liposomes except for the step for binding antibody.

5.3. Measurement of lipid concentration

The content of lipid in liposomes was determined as total cholesterol in the presence of 0.5% TritonX-100 with a Determiner TC555 kit (Kyowa) and the total amount of fatty acids was calculated from the molar ratio of each lipid.

5.4. Measurement of particle size and ζ-potential

The liposome solution was diluted 50 times with distilled water and size distribution and ζ-potentials of liposome particles were measured at 25°C using Zetasizer Nano-S90 (Malvern).

5.5. Quantification of antibody conjugated to the liposome

The amount of anti-E-selectin antibody on the surface of the liposome was measured by enzyme-linked immunosorbent assay (ELISA). Human E-selectin-Fc Chimera (R&D systems) was dissolved in the PBS (pH 7.2) to a final concentration of 2 mg/ml. Fifty microliters of the solution was added to each well of a 96-well plate (Falcon 3072, Falcon) and maintained at 25°C for 1 h for immobilization. After discarding the solution of each well, 300 μl of PBS containing 2% bovine serum albumin (BSA) was added to each well for blocking and incubated at 25°C for 2 h. Each well was then washed three times with PBS. Two milligrams per milliliter of anti-E-selectin antibody was diluted with PBS to a final concentration of 2.4, 1.2, 0.6 or 0.3 μg/ml (standard solution). One hundred microliters of standard solution and liposomes with anti-E-selectin antibody were added to each well of a 96-well plate and incubated at 25°C. After 1 h, the solution of each well was discarded and the well was washed three times with PBS. Next, 100 μl of anti-mouse IgG goat antibody which was labeled with HRP (Santa Cruz Biotechnology) diluted 8000-fold with PBS containing 10% Tween20, and 9% EDTA was added to each well and stood at 25°C for 1 h. After three washes with PBS, 100 μl of TMB Stabilized Substrate for HRP (Promega) was added to each well and reacted at 25°C for 20 min. Each well was then washed three times with PBS and 100 μl of 2 M sulfuric acid was added to each well to stop the reaction. The absorbances of standards and samples were measured at 405 nm using a microplate-reader (BioRad). The binding reactions of antibody were repeated three times and the results were expressed as mean ± SD.

5.6. Detection of E-selectin expressed on HUVEC

Ehrlich ascites tumor cells (CCL-77, ATCC) were cultured in DMEM (Sigma) supplemented with 10% fetal bovine serum (Biowest), 1 mg/ml streptomycin (Sigma) and 100 U/ml penicillin (Sigma) at 37°C in a humidified atmosphere of 5% CO_2 and air. The conditioned medium from EAT cells at 100% confluence was prepared and used as described below. Human umbilical vein endothelial cells (D&S Pharma) were cultured in a medium recommended for HUVEC (Medium for HUVEC, D&S Pharma). To each well of a 12-well plate, 1×10^5 cells of HUVEC in 500 μl medium were added and cultured at 37°C under 5% CO_2. To determine whether E-selectin is induced on the surface of HUVEC by the culture supernatant of the EAT cells, 500 μl of EAT conditioned medium (100% confluent) was added to HUVEC and cultured for 4 h. To induce E-selectin on HUVEC as a positive control, human TNF-α (R&D Systems) was added to a final concentration of 10 ng/ml and HUVEC were cultured for 4 h. As a negative control, 500 μl of DMEM supplement with 1 mg/ml streptomycin, 100 U/ml penicillin and 10% FBS was added to HUVEC and cultured for 4 h. The cells were washed with PBS and fixed with 3.7% formaldehyde for 10 min at 25°C. After washing with PBS containing 0.1% TritonX-100, 500 μl of PBS containing 0.1% BSA was added for blocking to the cells and incubated for 20 min at 25°C. The cells were then incubated in 10 μg/ml of anti-E-selectin monoclonal antibody at 25°C for 1 h. After washing with PBS, FITC labeled anti-mouse IgG antibody (Santa Cruz), which was diluted with 0.1% BSA (final concentration 5 μg/ml), was added and reacted for 1 h at 25°C. To stain for actin filaments, the cells were washed with PBS and incubated in 5 U/ml of rhodamine phalloidin solution (Molecular probes) at 25°C

for 20 min. After washing with PBS and distilled water, HUVEC were analyzed with a fluorescence microscope (CKX41, Olympus).

5.7. E-selectin targeting in vitro

Liposomes encapsulating Cy3 were used through these experiments. Ten microliters of liposomes conjugated with 3.9 μg of anti-E-selectin antibody per milligram of lipid was added to the wells of a 12-well plate containing HUVEC and incubated at 37°C for 30 min under 5% CO_2. After washing three times with PBS, 500 μl of medium was added to each well and incubated for 3 h. Liposomes without antibody were used as negative control. Binding inhibition was carried out to demonstrate that the binding of liposomes to HUVEC was antigen specific. To block the E-selectin on the cells, 100 μg of unlabeled anti-E-selectin monoclonal antibody was added to HUVEC expressing E-selectin. After washing three times with PBS, 500 μl of medium for HUVEC was added. Then, 10 μl of Cy3 encapsulated liposomes with anti-E-selectin antibody (3.9 μg antibody/mg lipid) was added to each well and incubated for 30 min. Each well was then washed three times with PBS and the cells were analyzed using a fluorescence microscope (CKX41, Olympus).

5.8. Detection of E-selectin in vascular vessel of solid EAT section

EAT cells (5×10^6 cells/mouse) were transplanted subcutaneously in the back of female BALB/c nude mice. After 10 days, tumors were excised and fixed in 10% neutral formalin solution (Wako) for 24 h. After fixation, the tissues were dehydrated, cleared, infiltrated and then embedded with paraffin. Then 4 μm thick sections were cut for hematoxylin and eosin staining and for immunohistochemistry. For double staining with fluorescence labeled antibodies, sections were deparafinized and stained as following. After blocking with 10% goat serum containing 3% TritonX-100 for 1 h at room temperature, sections were incubated with anti-E-selectin antibody (10 μg/ml) for 1 h at 37°C and then rinsed three times in PBS for 5 min each. Sections were further incubated with goat anti-mouse FITC labeled IgG antibody (Santa Cruz) diluting 200 times and Texas red conjugated *Lycopersicon esculentum* (tomato) lectin (Vector) diluting 100 times for 1 h at room temperature in dark and then rinsed three times in PBS for 5 min each in dark. The sections were mounted with glycerol-PBS (9:1) and then observed with an Olympus IX81 microscope equipped with a reflected light fluorescence device (Olympus).

5.9. E-selectin targeting in vivo

Liposomes encapsulating Cy5.5 were used throughout this experiment. EAT cells (5×10^6 cells/mouse) were transplanted subcutaneously to the right femoral region or to the right side in the back of female BALB/c mice (6 weeks old), and used for experiments 10 days later. To optimize the amount of antibody, 200 μl of liposomes conjugated with various amount of anti-E-selectin antibody was injected via the tail vein. Then photon count per second of Cy5.5 in the tumor at the right femoral region of the same mouse was measured with eXplore Optix (excitation at 680 nm and emission at 700 nm; GE Healthcare), under isoflurane anesthesia before and after injection. Three mice were used in each experimental group. The results of photon counts per second are expressed as mean ± SD. For *in vivo* imaging, 200 μl of liposomes conjugated with 3.9 μg of anti-E-selectin antibody/mg lipid was injected from the tail vein. Simultaneously, 200 μl of liposomes conjugated with normal porcine IgG (Sigma) and liposomes without antibody were injected as control. The signal of Cy5.5 in the tumor transplanted at the right side in back of mouse was monitored under isoflurane anesthesia with IVIS Lumina-II (excitation at 680 nm and emission at 700 nm; Caliper Life Sciences).

All animal experiments through this study were conducted in full compliance with local, national, ethical and regulatory principles for animal care.

Acknowledgements

We thank Dr David S. Salomon (NCI, Bethesda, MD, USA) for reading this manuscript and for enthusiastic discussions and suggestions.

REFERENCES

1. Frangioni JV. In vivo near-infrared fluorescence imaging. Curr Opin Chem Biol 2003; 7: 626–634.
2. Maruyama K, Yuda T, Okamoto A, Kojima S, Suginaka A, Iwatsuru M. Prolonged circulation time *in vivo* of large unilamellar liposomes composed of distearoyl phosphatidylcholine and cholesterol containing amphipathic poly (ethylene glycol). Biochim Biophys Acta 1992; 1128: 44–49.
3. Gabizon A, Papahadjopoulos D. Liposome formulation with prolonged circulation time in blood and enhanced uptake by tumors. PNAS 1988; 85: 6949–6953.
4. Vyas SP, Singh A, Sihorkar V. Ligand-receptor-mediated drug delivery: an emerging paradigm in cellular drug targeting. Crit Rev Ther Drug Carrier Syst 2001; 18: 1–76.
5. Willis M, Forssen E. Ligand-targeted liposomes. Adv Drug Deliv Rev 1998; 29: 249–271.
6. Kessner S, Krause A, Rothe U, Bendas G. Investigation of the cellular uptake of E-selectin-targeted immunoliposomes by activated human endothelial cells. Biochim Biophys Acta 2001; 1514: 177–190.
7. Klivanov AL, Maruyama K, Beckerleg AM, Torchilin VP, Huang L. Activity of amphipathic poly (ethylene glycol) 5000 to prolong the circulation time of liposomes depends on the liposome size and is unfavorable for immunoliposomes binding to target. Biochim Biophys Acta 1991; 1062: 142–148.
8. Bevilacqua MP, Stengelin S, Gimbrone MA, Seed B. Endothelial leukocyte adhesion molecule 1: an inducible receptor for neutrophils related to complement regulatory proteins and lectins. Science 1985; 243: 1160–1165.
9. Vestweber D, Blanks JE. Mechanisms that regulate the function of the selectins and their ligands. Physiol Rev 1999; 79: 181–213.
10. Mayer B. De novo expression of the cell adhesion molecule E-selectin on gastric cancer endothelium. Langenbeck's Arch Surg 1998; 383: 81–86.
11. Liu F, Rabinovich GA. Galectins as modulators tumor progression. Nature Rev Cancer 2005; 5: 29–41.
12. Pober JS, Bevilacqua MP, Mendrick DL, Lapierre LA, Fiers W, Gimbrone MA. Two distinct monokines, interleukin 1 and tumor necrosis factor, each idependently induce biosynthesis and transient expression of the same antigen on the surface of cultured human vascular endothelial cells. J Immunol 1986; 136: 1680–1687.
13. Kim I, Moon SO, Kim SH, Kim HJ, Koh YS, Koh GY. Vascular endothelial growth factor expression of intercellular adhesion molecule 1 (ICAM-1), vascular cell adhesion molecule 1 (VCAM-1), and E-selectin through nuclear factor-kappa B activation in endothelial cells. J Biol Chem 2001; 276: 7614–7620.
14. Ehrhardt C, Kneuer C, Bakowsky U. Selectin – an emerging target for drug delivery. Adv. Drug Deliv 2004; 56: 527–549.
15. Dodd RB, Drickamer K. Lectin-like proteins in model organisms: implications for evolution of carbohydrate-binding activity. Glycobiology 2001; 11: 71R–79R.
16. Kilpatrick DC. Animal lectins: a historical introduction and overview. Biochim Biophys Acta 2002; 1572: 187–197.

17. Spragg DD, Alford DR, Greferath R, Larsen CE, Lee KD, Gurtner GC, Cybulsky MI, Tosi PF, Nicolau C. Immunotargeting of liposomes to activated vascular endothelial cells; A strategy for site-selective delivery in the cardiovascular systems. Proc Natl Acad Sci USA 1997; 94: 8795–8800.
18. Stahn R, Grittner C, Zeisig R, Karsten U, Felix SB, Wenzel K. Sialyl Lewis (X)–liposomes as vehicles for site-directed, E-selectin-mediated drug transfer into activated endothelial cells. Cell Mol Life Sci 2001; 58: 141–147.
19. Tan PH, Manunta M, Ardjomand N, Xue SA, Larkin DF, Haskard DO, Taylor KM, George AJ. Antibody targeted gene transfer to endothelium. J Gene Med 2003; 5: 311–323.
20. Zeising R, Stahn R, Wenzel K, Behrens D, Fichtner I. Effect of sialyl LewisX-glycoliposomes on the inhibition of E-selectin-mediated tumor cell adhesion *in vitro*. Biochim Biophys Acta 2004; 1660: 31–40.
21. Murphy TJ, Thurston G, Ezaki T, McDonald DM. Endothelial cell heterogeneity in venules of mouse airways induced by polarized inflammatory stimulus. Am J Pathol 1999; 155: 93–103.
22. Hirai M, Minematsu H, Kondo N, Oie K, Igarashi K, Yamazaki N. Accumulation of liposome with Sialyl Lewis X to inflammation and tumor region: application to *in vivo* bio-imaging. Biochem Biophys Res Commun 2007; 353: 553–558.
23. Thomas VH, Yang Y, Rice KG. In vivo ligand specificity of E-selectin binding to multivalent sialyl LewisX N-Linked oligosaccharides. J Biol Chem 1999; 274: 19035–19040.
24. Yamazaki N, Kojima S, Yokoyama H. Biomedical nanotechnology for active drug delivery systems by applying sugar-chain molecular functions. Curr Appl Phys 2005; 5: 112–117.
25. Yamazaki N. Analysis of the carbohydrate-binding specificity of lectin-conjugated lipid vesicles which interact with polysaccharide fragment. J Membr Sci 1989; 41: 249–267.
26. Yamazaki N, Kodama M, Gabius H-J. Neoglycoprotein–liposome and lectin–liposome conjugates as tools for carbohydrate recognition research. Meth Enzymol 1994; 242: 56–65.
27. Hashida N, Ohguro N, Yamazaki N, Arakawa Y, Oiki E, Mashimo H, Kurikawa N, Tano Y. High-efficacy site-directed drug delivery system using Sialyl–Lewis X conjugate liposome. Exp Eye Res 2008; 86: 138–149.
28. Van Kasteren SI, Campbell SJ, Serres S, Anthony DC, et al. Glyconanoparticles allow pre-symptomatic *in vivo* imaging of brain disease. Proc Natl Acad Sci 2009; 106: 18–23.
29. Coussens LM, Web Z. Inflammation and cancer. Nature 2002; 420: 860–867.
30. Sawa Y, Tsuruga E. The expression of E-selectin and chemokines in the cultured human lymphatic endothelium with lipopolysaccharides. J Anat 2008; 212: 654–663.

International Journal of Pharmaceutics 391 (2010) 274–283

Contents lists available at ScienceDirect

International Journal of Pharmaceutics

journal homepage: www.elsevier.com/locate/ijpharm

Pharmaceutical Nanotechnology

Novel and simple loading procedure of cisplatin into liposomes and targeting tumor endothelial cells

M. Hirai[a,b], H. Minematsu[a], Y. Hiramatsu[a], H. Kitagawa[a], T. Otani[a,b], S. Iwashita[a], T. Kudoh[b], L. Chen[b], Y. Li[b], M. Okada[b], D.S. Salomon[c], K. Igarashi[a], M. Chikuma[d], M. Seno[b,*]

[a] R&D Division, Katayama Chemical Industries Co., LTD, Minoh, Osaka 562-0015, Japan
[b] Department of Medical and Bioengineering Science, Graduate School of Natural Science and Technology, Okayama University, Okayama 700-8530, Japan
[c] Tumor Growth Factor Section, Mammary Biology and Tumorigenesis Laboratory, Center for Cancer Research, National Cancer Institute, Bethesda, MD 20892, USA
[d] Osaka University of Pharmaceutical Sciences, Takatsuki, Osaka 569-109, Japan

ARTICLE INFO

Article history:
Received 20 August 2009
Received in revised form 1 January 2010
Accepted 27 February 2010
Available online 6 March 2010

Keywords:
Cisplatin
Cis-diamminedinitratoplatinum (II)
Liposome
E-selectin
Sialyl Lewis^X

ABSTRACT

Although intravenous administration of high levels of cisplatin (CDDP) are limited due to its severe side effects, efficient delivery of CDDP directly to the tumor should improve the therapeutic response while potentially by-passing significant side effects.

High loading of CDDP into liposomes is one technique that could be used as a potential drug delivery system. Since *cis*-diamminedinitratoplatinum (CDDP3) is highly soluble in water and converts to CDDP in the presence of chloride ions, we encapsulated CDDP3 into liposomes in the absence of chloride ions and supplemented chloride ions to prepare CDDP-encapsulated liposomes (CDDP-Lip) resulting in a significantly improved loading efficiency of CDDP. We further conjugated the CDDP-Lip with Sialyl Lewis^X (CDDP-SLX-Lip) because we previously demonstrated Sialyl Lewis^X enhanced efficient accumulation of liposomes into tumors in vivo. CDDP-SLX-Lip treated mice showed a survival rate of 75% at 14 days even if a lethal level of CDDP was injected into mice. Loss of body weight was negligible and no histological abnormality was found in a variety of normal tissues. Accumulation of CDDP-SLX-Lip was about 6 times more than that of CDDP-Lip or CDDP. As the result, there was better antitumor activity of CDDP-SLX-Lip than that of CDDP-Lip with significantly less toxic effects in normal tissues.

1. Introduction

Cisplatin (*cis*-diamminedichloroplatinum, CDDP) is one of the most widely used chemotherapeutic drugs in the clinical treatment of a variety of tumors, such as lung, ovarian and gastric carcinomas (Comis, 1994). However, administration of escalating doses of CDDP is limited because of severe side effects such as nephrotoxicity, hematopoietic injury, and deafness (Cvitkovic et al., 1977; Hayes et al., 1977; Von Hoff et al., 1979; Goldstein et al., 1981). Efforts to decrease these deleterious side effects by screening various CDDP derivatives and by developing improved forms of dosage or methods of medication have been unsuccessful (Borch and Markman, 1989; Ogilvie et al., 1992; Legha et al., 1992; Navari et al., 1994). Practical drug delivery systems, which specifically recognize tumors to efficiently deliver drugs at high doses *in vivo*, have also been undertaken. However, as yet no efficient carriers to efficiently deliver CDDP to tumors have been developed (Bandak et al., 1999; Newman et al., 1999; Vaage et al., 1999). Among the several liposomal formulations of CDDP, the latest is SPI-077, in which CDDP is encapsulated in pegylated stealth liposomes (Newman et al., 1999). Although preclinical studies showed that compared with the free drug, SPI-077 exhibited improved stability, prolonged circulation time, increased antitumor effect, and reduced side effects (Newman et al., 1999; Vaage et al., 1999), little antitumor activity of SPI-077 was observed in Phase I/II studies (Harrington et al., 2001; Kim et al., 2001; Veal et al., 2001). The major problem of conventional liposomal formulations involving CDDP, such as in SPI-077, was the extremely low drug to lipid weight ratio due to water insolubility and low lipophilicity of CDDP, which resulted in failure to adequately deliver the drug to the tumor (Bandak et al., 1999; Meerum Terwogt et al., 2002).

In contrast with CDDP, *cis*-diamminedinitratoplatinum (II) (CDDP3), one of the various CDDP derivatives, is highly water soluble and is readily converted into CDDP in the presence of chloride

Abbreviations: SLX, Sialyl Lewis^X; CDDP, *cis*-diamminedichloroplatinum (II) or cisplatin; CDDP3, *cis*-diamminedinitratoplatinum (II); SLX-Lip, liposomes modified with SLX; CDDP-Lip, liposomes containing CDDP; CDDP-SLX-Lip, liposomes modified with SLX containing CDDP; LEL, *lycopersicon esculentum* lectin.

* Corresponding author at: Room 361, Bldg. ENG-6, Laboratory of Nano-Biotechnology, Department of Medical and Bioengineering Science, Graduate School of Natural Science and Technology, Okayama University, 3.1.1 Tsushima-Naka, Kita-ku, Okayama 700-8530, Japan. Tel.: +81 86 251 8216; fax: +81 86 251 8216.
E-mail address: mseno@cc.okayama-u.ac.jp (M. Seno).

0378-5173/$ – see front matter © 2010 Elsevier B.V. All rights reserved.
doi:10.1016/j.ijpharm.2010.02.030